Segmentation-based Wireframe Generation for Parametric Modeling of Human Body Shapes

Jida Huang
Mechanical and Industrial Engineering
University of Illinois at Chicago
Chicago, Illinois 60607
Email: jida@uic.edu

Tsz-Ho Kwok*
Mechanical, Industrial and Aerospace Engineering
Concordia University
Montreal, QC H3G 1M8, Canada
Email: tszho.kwok@concordia.ca

Wireframes have been proved useful as an intermediate layer of the neural network to learn the relationship between the human body and semantic parameters. However, the definition of the wireframe needs to have anthropological meaning and is highly dependent on experts' experience. Hence, it is usually not easy to obtain a well-defined wireframe for a new set of shapes in available databases. An automated wireframe generation method would help relieve the need for the manual anthropometric definition to overcome such difficulty. One way to find such an automated wireframe generation method is to apply segmentation to divide the models into small mesh patches. Nevertheless, different segmentation approaches could have various segmented patches, thus resulting in various wireframes. How do these different sets of wireframes affect learning performance? In this paper, we attempt to answer this research question by defining several critical quantitative estimators to evaluate different wireframes' learning performance. To find how such estimators influence wireframe-assisted learning accuracy, we conduct experiments by comparing different segmentation methods on human body shapes. We summarized several meaningful design guidelines for developing an automatic wireframe-aware segmentation method for human body learning with such verification.

1 Introduction

The synthesis of the human body model is widely used in various types of applications such as the fashion industry [1], medical [2], and wearable products [3]. An accurate and robust synthesis method for human body modeling is critical prior to these applications. In order to find such a human body synthesis method, many works have studied the statistics of the human shape database [4,5]. To improve the accuracy and robustness of the human model synthesizing from semantic parameters [6], the concept of applying feature wireframe in the learning is introduced [7]. The wireframe is defined as a set of feature curves on the human body model based on the anthropometric rules. Such a feature wireframe has proved to be useful for decomposing the original complex problem into solvable sub-problems. Nevertheless, anthropometric experts usually define the wireframe manually, which is highly dependent on the experience, and it is usually not available to acquire such wireframes when a new dataset is available. As a result, an automatic wireframe generation method for a set of models is highly preferred, especially when three-dimensional (3D) scanning devices become ubiquitous nowadays.

To find such an automatic feature wireframe generation method, we rethink the wireframe's role on the human body shape. In [7], the defined wireframe is used to separate the whole human body into small mesh patches so that the learning can focus on each mesh patch, and the original learning problem can be decomposed to two levels of relationship: from the parameters to the wireframe and from the wireframe to the mesh. In other words, the wireframe serves a function to decompose the human model into small components. This is very similar to the mesh segmentation approach, which aims to partition a 3D mesh into sub-meshes. Since mesh segmentation is a well-studied problem in computer graphics, and many automatic segmentation methods have been developed [8,9], the objective here is to apply segmentation to generate the wireframe. Specifically, when a human shape is segmented into different partitions, the boundaries between these partitions can be used as the feature wireframe. In this way, an automated wireframe generation method can be developed utilizing the mesh segmentation approach.

---

*Corresponding Author.

Different segmentation approaches will lead to different segmented results and resulting wireframes. As the wireframe serves an intermediate layer role in the learning framework, it is crucial to understand how different wireframes would affect the learning performance. To allow the development and optimization of an automatic wireframe generation for semantic learning, we define a set of quantitative factors and investigate their relationship to the learning performance. We have formulated hypotheses on the quantitative criteria for applying the segmentation method to wireframe generation. To test these hypotheses, various segmentation approaches with distinct properties are selected, and the correlation between the extracted criteria and learning performance is studied. From experimental results, we find how the criteria are beneficial to improving the learning performance when developing an automated wireframe generation method by using segmentation. Based on this, we summarize several design guidelines for the automatic learning-aware feature wireframe generation. Thus, the main contributions of this paper are summarized as follows.

1. The mesh segmentation is utilized for the feature wireframe construction, and a segmentation-based feature wireframe generation framework is proposed for human body learning.
2. A set of quantitative factors affecting the learning performance are defined, and the corresponding hypotheses are proposed based on such factors.
3. The proposed factors are verified with the comparison of different wireframes generated from various segmentation approaches, and their effects on the learning performance are studied.
4. From the correlation study between the proposed factors and the learning performance, several wireframe design criteria are concluded for developing an automated way of wireframe generation.

This paper is organized as follows. The rest of this section reviews some related works and briefly introduces the wireframe-based learning framework. Section 2 gives an overview of the segmentation-based wireframe generation methodology. The quantitative estimators for the learning performance as well as the segmentation methods selected to test the hypotheses are presented in Section 3. The experimental results are reported in Section 4, and they are discussed in Section 5. Finally, Section 6 concludes the paper.

1.1 Literature review

Human body modeling is one of the fundamental problems in the computer graphics area. Previous works studied the human body modeling mainly based on the statistical properties of an available dataset of human body models [4, 10–12]. Recent works [13, 14] tried using the parameterization approach for the modeling task. For example, automatic modeling of human bodies from sizing parameters was studied in [15]; and a feature-based parameterization modeling method from the unorganized point cloud was presented in [16]. This method was further optimized with cross
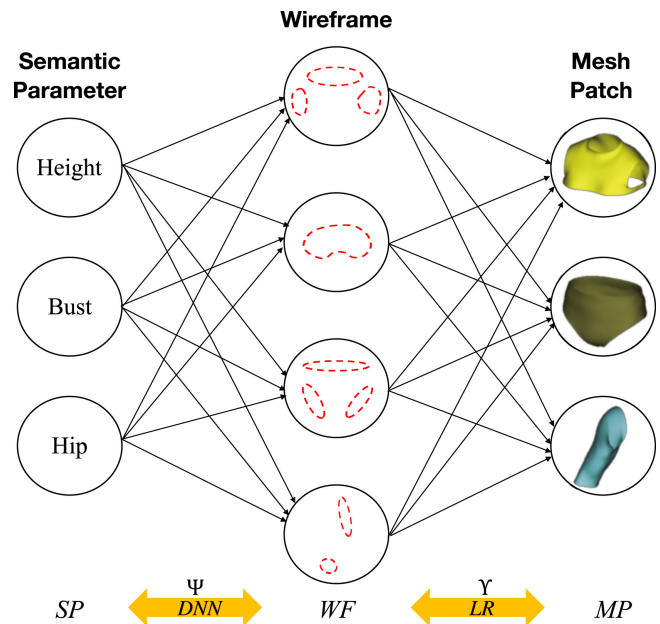
Fig. 1: The wireframe-assisted semantic learning methodology. Reprinted from [7], with permission from Elsevier.

parameterization in [17]. In [18], a tensor decomposition-based method was developed for modeling 3D human body with variations on both human shape and pose. While in [19], an example-guided, anthropometry-based modeling method was proposed for creating 3D human body models, and took partial anthropometric measurements of users as the input. Most of these methods relied on the available human shape dataset and represent the human shape with a group of anthropocentric parameters. To utilize such parameters for the human body modeling, generating the human shape from semantic parameters was studied in [6]. It has been demonstrated that such a generation process could lose important information and affect the modeling quality. However, this issue can be relieved mainly by introducing a set of defined wireframes on the human shape model [7]. Thus the generation of the wireframe is the focus of this paper.

1.2 Wireframe-assisted human body learning

To be self-contained, the wireframe-assisted human body learning method [7] is briefly summarized here. The principle workflow of the method is illustrated as in Fig. 1. There are three primary layers in the learning method: semantic parameters (SP), feature wireframe (WF), and mesh patches (MP). By introducing the WF layer, the human model is separated by the wireframe into K patches. The wireframe can then be separated into K sets accordingly, each of which is the feature curves that are interpolated by the corresponding patch, i.e., the patch's boundary. In this framework, two correlations need to be learned: $SP \rightarrow WF$, and $WF \rightarrow MP$. These two correlations are acquired through a deep neural network (DNN) and a linear regression (LR).
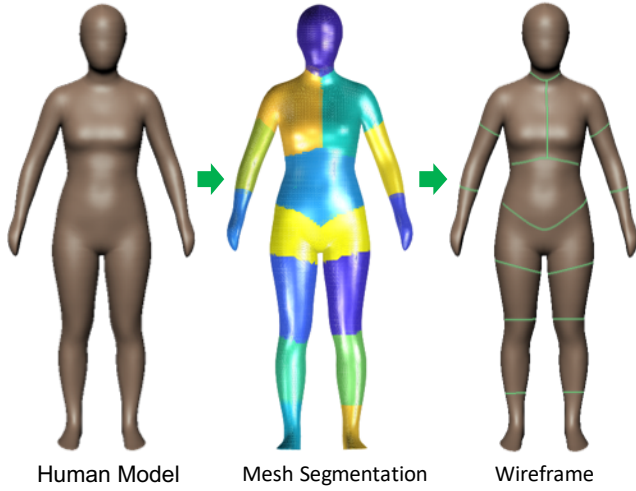
Fig. 2: Segmentation-based wireframe generation

Specifically, the relations are modeled as follows:

$$WF = \Psi(SP, \psi).$$
$$mp_k = \Upsilon_k(wf_k, \upsilon_k), \qquad (1)$$
$$\text{where} \quad wf_k \in WF, \quad mp_k \in MP \quad (k = 1, \ldots, K).$$

Ψ and Υ_k represent the two learning relations of DNN and LR, while ψ and υ_k are the vectors of unknown variables that need to be solved. wf and mp are the sets of separated wireframes and patches, and K is the number of separated patches. In practice, to extract the most important components from the data for the learning, a principal component analysis (PCA) is first applied separately to SP, WF as well as each mp_k and wf_k.

By dividing the whole learning problem into subproblems, the proposed method can avoid losing feature information of the human shape model and is much faster by solving smaller sub-problems with wireframe assistance. Therefore, in this framework, the critical step is the definition of the wireframes. Since such a wireframe can capture a human body's features and affect the relations of separated mesh patches and their boundaries, it is pivotal to determine a set well-defined wireframe to separate the human model properly. Thus the divided sub-problem can be easily studied, i.e., the learning performance of the hierarchy method described as in Fig. 1 can be secured. The anthropocentric rules were used to define the wireframe [7], and this paper aims to automate it by using segmentation.

2 Segmentation-Based Wireframe Generation

The overview of the proposed segmentation-based wireframe generation is illustrated as in Fig. 2. Although only one model is shown in the figure, it represents a set of human body models. There exists a bijective mapping among all the models, i.e., their meshes have the same connectivity and the same number of vertices with correspondences, but just the vertex positions are different. Therefore, when one

model is segmented, the results can be directly transferred to all the other models consistently. After segmentation, the boundary of the segmented patches is extracted as the wireframe of the human shape. Due to the nature of segmentation methods, the extracted boundary may not be smooth and have jagged shapes. Hence, a post-processing step is introduced to smooth the boundaries. After that, the wireframe is procured for the learning. The technical details of these steps are presented in the following.

2.1 Mesh segmentation

Mesh segmentation has been a classical fundamental problem in geometry processing and computer graphics. The objective of segmentation methods is to decompose the whole mesh into small regions. Typically, the mesh is represented with a triangulated mesh, which is defined as $\mathcal{M} = (V, E, F)$, where V, E, and F are the vertices, edges, and faces of the mesh model respectively. A standard segmentation partitions $\mathcal{M}$ with K disjoint subsets $\mathcal{P}_1, \ldots \mathcal{P}_K \in \mathcal{M}$, where $\mathcal{P}_k$ is a subset of vertices $\mathcal{P}_k \in V$. Two patches $\mathcal{P}_i$ and $\mathcal{P}_j$ are neighbours if they contain vertices $\exists i \in \mathcal{P}_i$ and $\exists j \in \mathcal{P}_j$ that are connected by an edge $\{i, j\} \in E$. The partitioning process is usually implemented through a clustering method by defining a similarity or distance function $\mathcal{D}$ for adjacent vertices or faces, as follows:

$$\mathbf{x} = \arg\min \sum_{k=1}^{K} \sum_{x_i, x_j \in \mathcal{P}_k} \mathcal{D}(x_i, x_j), \quad i \neq j,$$

where $\mathbf{x}$ is the optimal segmentation, x_i and x_j are the vertices or faces on the mesh $\mathcal{M}$. Different segmentation methods include distinct clustering principles [20–24]. The readers are referred to two recent survey papers [8, 9] for the classification of these clustering principles. An example is shown in Fig. 2 (middle). In this paper, the mesh segmentation is mainly used for generating the wireframe on the human model. It is expected that the segmenting principle can produce the wireframes which are amiable for improving the learning performance on human body shape. Therefore, a clustering method that can find a set of meaningful wireframes similar to the anthropocentric one is preferred. Thus, to develop an automated segmentation-based wireframe generation method, the main focus of this paper is to explore the inherent factors that bridge the segmenting principle and the wireframe-assisted learning performance.

2.2 Wireframe smoothing

Since segmentation results are the clusters of triangle faces, the boundaries of these clusters usually are rough due to the triangles. To obtain smooth wireframes, a Laplacian smoothing operation [25] is applied to the segment boundaries on the triangulated surface. The smoothing process is illustrated in Fig. 3. In each iteration, a vertex v on the wireframe is moved along a direction to shorten the length between its predecessor vertex v_- and successor vertex v_+ (Fig. 3a). To preserve the shape as much as possible, the new

3
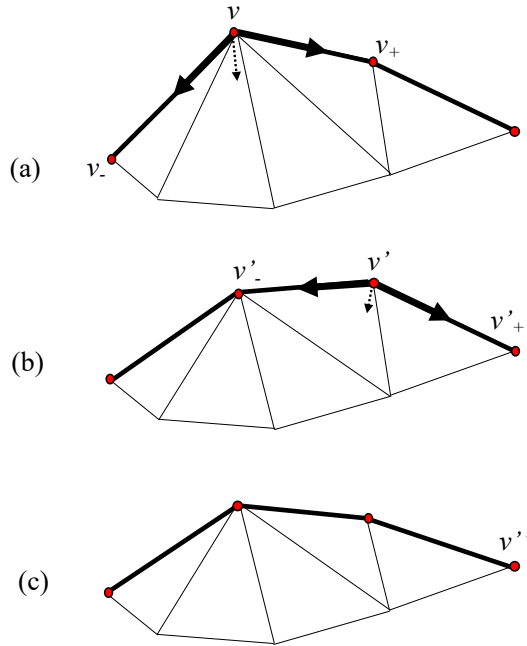
Fig. 3: Illustration of smoothing the wireframe (bold curve). (a) In each operation, a vertex v is moved on the surface to shorten the curve length between its predecessor and successor vertices: v_- and v_+. (b) The operation is applied to every vertex on the wireframe subsequently. (c) The smoothed wireframe is obtained.

position is restricted to be on the original surface. After updating v, its successor vertex v_+ becomes the next vertex v' to be updated (Fig. 3b), and this operator is applied to all vertices on the wireframe in one iteration. Through several (5 in this paper) iterations of this Laplacian smoothing, the wireframe are smoothed. In this way, the topology of the mesh is not altered but just the vertex positions, and thus it can be conducted on all models separately after segmentation. Once this smoothing process is finished, the wireframes can then be used for semantic learning. Note that the smoothing operation is directly conducted to wireframes on the whole surface, and the wireframe in Fig. 2 is already smoothed.

3   Characterization Methodology

In our proposed segmentation-based wireframe generation framework, the wireframe is coming from the automation segmenting principles. Simultaneously, the primary purpose of the segmentation method is to separate the input mesh into small regions with similar geometric features, e.g., curvature, normal, and convexity. It does not consider the effects on the generated wireframe and the corresponding learning performance. Therefore, to evaluate the learning performance of wireframes generated from different segmenting principles, a set of quantifiable criteria must be established. Different segmentation approaches would lead to diverse wireframes. How would the segmenting principles involved in these approaches affect learning performance? This is the main research question we want to investigate for the segmentation-based wireframe generation. To fairly

evaluate multifarious wireframes' learning performance, we quantitatively extract the standard comparable criteria and factors of the wireframe. Then we propose a set of hypotheses based on these characteristics that may influence the learning performance.

3.1   Quantifiable criterion of the wireframe

To establish the wireframe's quantifiable criteria that may affect the relation learning performance, the features of the wireframe are examined, and the standard statistical attributes of these features are extracted in this section.

3.1.1   Number of points on wireframe and mesh patches

One of the essential attributes in statistical learning is the dimensions of inputs and outputs. When there is an imbalance between the data, the problem becomes either over-determined or under-determined. In the parametric learning framework, the wireframe separates the human shape into small mesh patches. The relation (Υ_k) between the mesh patches (mp_k) and their corresponding boundary wireframes (wf_k) is learnt through Eq.(1). Therefore, the inputs and the outputs are the positions of the points on the wireframe and the mesh patch. More accurately, it should be their principal components (PCs) since PCA is applied before learning. It is expected that these two dimensions to be close so that the impact of dimensional imbalance can be minimized, and hopefully, the learning performance is improved. As such, we have the following hypothesis.

Hypothesis 1: *The dimension ratio of boundary wireframe (wf_k) to mesh patch (mp_k) in a segmented mesh patch is better to be close to one.*

Note that this measurement can also be applied to the relation Ψ between SP and WF. However, SP to WF only has one ratio for one segmentation method on one number of resulting mesh patches. It may not be fair and is statistically invalid to compare different segmenting methods on this ratio, so it is not studied in the paper.

3.1.2   Smoothness of the wireframe

The wireframes are the boundary of the mesh patches, and it is expected that the boundary wireframes can depict the outline and represent the shape profile of the bounded patches. While the segmentation approaches separate the human shape with an automatically segmenting rule, the generated wireframes may contain irregular curves even after boundary smoothing. This is like the statistical noises in signal processing. If a boundary wireframe includes such noises due to the curves' non-smoothness, the noises may disturb the learning process. Therefore, we propose another hypothesis.

Hypothesis 2: *A smoother boundary wireframe is beneficial to the learning performance.*

To quantitatively measure the boundary wireframes' smoothness, the integral of absolute Gaussian curvature is applied as the smoothness measurement for each closed
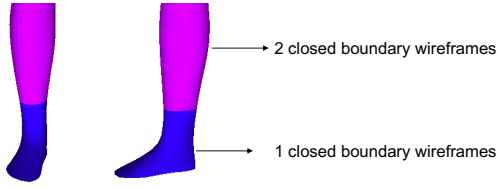
Fig. 4: Illustration of the topology of segmented mesh patches.

curve on the boundary wireframes of a mesh patch. Since the representation of the human shape is in a triangulated format, the average point curvature on the wireframes is used to indicate the smoothness of the wireframe wf_k:

$$s_k = \frac{1}{n_k} \sum_{i=1}^{n_k} \kappa_i, \tag{2}$$

where s_k is the smoothness measure of wireframe wf_k, κ_i is the Gaussian curvature of ith vertex on the wireframe, and n_k is the total number of vertices on the wireframe wf_k. It is expected that the value s_k is the smaller the better.

3.1.3 Topology of mesh patches

Topology refers to an object's inherent structural connectivity, and it is often described by the genus number. One way to classify models into topological classes is to count the number of holes contained in shape. When the wireframes segment the human shape into disparate mesh patches, each patch could contain one or more boundary wireframe loops. Figure 4 is an example demonstrating how to use the number of closed rings to represent the topology of segmented mesh patches, i.e., if a mesh patch has one boundary wireframe, its genus number is equal to one. These loops act as handles to describe the whole mesh patch, and thus they can reflect the complexity of the shape geometry within the mesh patch. A larger number of closed rings means that a mesh patch has more handles, which can depict the contour of the bounded shape geometry, and thus it may be easier for the learning of the relations between the boundary wireframe and mesh patch. Based on this observation, we have the following hypothesis.

Hypothesis 3: The larger genus number (i.e., the number of closed boundary wireframes) of a mesh patch, the more effective in learning its geometry.

3.1.4 Uniformity of mesh patches

Previous criteria are mostly related to the learning performance in individual mesh patches, and here we also want to look into how the distribution of data would affect the learning. The wireframe partitions the human shape into various mesh patches and the resulted patches would have distinct shapes and sizes. This variety would affect the learning of both relations (Ψ and Υ_k). For example, if the patches have significantly distinctive sizes, the results would be weighted

more heavily on one than another. Although some patches may be learned better, the others may be worse. Uniformly distributing the data may help to reduce such variety, and we have the following hypothesis.

Hypothesis 4: The segmentation being more uniform improves the overall quality of parametric modeling.

We use the following uniformity measuring method for all segmented mesh patches.

$$uni(mp_1, mp_2, ..., mp_K) = \frac{1}{\sqrt{K-1}} \times \frac{stdev_k(size(mp_k))}{mean_k(size(mp_k))}, \tag{3}$$

where K is the number of mesh patches segmented by the wireframe, and $size(mp_k)$ returns the size of patch mp_k, which is the sum of areas for all faces inside the mesh patch. The coefficient of variation is a standardized measure of dispersion and thus provides a scale-invariant uniformity index. According to this uniformity estimation, if the sizes of segmented mesh patches are close, the variety would be small. Thus the value is expected to be the smaller, the better.

3.2 Segmentation methods

There is an enormous amount of literature on mesh segmentation approaches developed based on the different types of segmenting principles [8,9]. This paper aims to find which segmenting rule can generate wireframes beneficial to the relations learning on human shape. To test the hypotheses in the previous section, we select four segmentation approaches mainly based on the discussed quantifiable criteria such as curvature and uniformity that may affect the relations learning. They are curvature-based, uniformity-based, convexity-based, and consensus segmentation. These four approaches segment the input human shape according to the clustering of different features. Such various features would generate distinctive wireframes and further affect the learning performance. Then we could explore how the features influence the aforementioned criteria and find out which factors are beneficial to the wireframe-assisted learning by employing a comparative study of the generated wireframe. The four segmentation approaches are visualized in Fig. 5, and the details of each method are briefly introduced as follows.

3.2.1 Curvature-based segmentation

The first selected approach is a curvature-based segmentation [26]. The main reason to select such a curvature-based method is to provide homogeneous segments for input human shape w.r.t. the predetermined curvature. Besides, it can affect the smoothness of the generated wireframe. The selected method [26] combines the Fast Machining [27] and Farthest Point Sampling [28], which is named FMFPS here for simplicity. FMFPS is implemented based on sampling seed points and updating a Voronoi diagram, equivalent to segmenting the sampling domain, i.e., assigning the labels (segmented region number) for each input point. To deter-

Fig. 5: Illustration of different segmentation approaches with resulting 15 segments.

3.2.4 Consensus segmentation

Consensus segmentation tends to acquire a stable segmentation for the input shape. Here, a stable region detection (RRD) [33] method is applied for the wireframe generation. In the RRD method, firstly, a set of over-segmentation for the given shape is produced with random cut algorithm [34] as well as Global Point Signature (GPS) [35] clustering of vertices on the shape. After groups of initial segmentation are created, RRD uses an optimization algorithm to find the optimal consensus segmentation, which is defined as the segmentation is as close as possible to all the ones in the initial groups of ensemble segmentation. This means that the final detected segmentation is the most stable (consensus) one across the groups of initial segmentation. The details of this optimization procedure are referred to [33]. In this paper, implementation of RRD is reproduced and applied for generating the wireframes on the human shape.

4 Results

Based on the presented methodology, the results are reported in this section. The same database of the human body used in the previous work [7] is applied, which has 77 subjects of woman model. Each model contains 11,072 mesh vertices and has its corresponding defined semantic parameters. There are 8 semantic parameters used in the study, e.g., body height, neck girth, bust, and waist. To assess the learning performance, the first 67 subjects from the database are used for training, and the remaining ten subjects are used for testing. For the testing, the framework synthesizes the shape of the models using the ten human shapes' semantic parameters and compares the synthesized results with the actual models. The synthesis error is measured by comparing the distances between the corresponding vertices. Specifically, the synthesized human model error (err_h) is defined as

$$E_h = \|h, \hat{h}\|_2 = \sum_{i=1}^{n_h} \|\mathbf{x_i} - \hat{\mathbf{x}_i}\|_2, \quad \mathbf{x_i} \in h, \hat{\mathbf{x}_i} \in \hat{h}, \tag{4}$$

mine the stopping criterion, FMFPS formulates a cost function based on the shape's local curvatures that regulate an incremental and decremental strategy for the segmentation. The implementation of the FMFPS method [26] is reproduced in our experiments, and the Gaussian curvature is applied here.

3.2.2 Uniformity-based segmentation

Since one of the hypotheses is related to the uniformity of segmented mesh patches, we select a uniformity-based segmentation method that tends to segment the human shape into similar sizes. Specifically, we use the uniform patch growing algorithm [29] here. In this algorithm, K random vertex seeds are firstly generated, then the patches are grown by computing distances of neighbouring vertices to the corresponding seed, and the seeds are updated in the growing procedure. The uniformity metric is used as a stopping criterion for the growing. The implementation of [29] is reproduced and applied in our experiments.

3.2.3 Convexity-based segmentation

The convexity-based method tends to segment the shape into convex or nearly convex regions. In this type of method, the approximate convexity (AC) segmentation [30] is selected here. In the AC method, the shape is firstly decomposed into a large number of small and near-convex components by a spectral clustering of the vertex-connectivity graph. Then, the mutual visibility of adjacent patches is estimated as a merging criterion. After this initial merging, each patch's volumetric profile is computed with a shape diameter function (SDF) [31]. Based on their volumetric profiles, the patches are merged according to their similarity which is calculated based on the Earth Mover's Distance (EMD) [32], e.g., two adjacent patches with small EMD distance are likely to be merged together. Finally, a point-level graph cut optimization on the merged components is conducted to refine the segments' boundaries. The original implementation of [30] is applied here in our experiments.

where $\mathbf{x_i}$ and $\hat{\mathbf{x}_i}$ are the vertices from the original h and the synthesized $\hat{h}$ human models, and n_h is the number of the vertices on the human models. Similarly, the synthesis error can also be defined for each mesh patch to study how the boundary wireframe affects each patch's learning. Since the number of points among the mesh patches varies, the synthesis error of a mesh patch (err_{mp_k}) is averaged by the number of vertices to normalize the error:

$$E_{mp_k} = \frac{\|mp_k, \hat{mp}_k\|_2}{n_k} = \frac{\sum_{i=1}^{n_k} \|\mathbf{x_i} - \hat{\mathbf{x}_i}\|_2}{n_k}, \quad \mathbf{x_i} \in mp_k, \hat{\mathbf{x}_i} \in \hat{mp}_k \tag{5}$$

where mp_k is the original k^{th} mesh patch, $\hat{mp}_k$ is the predicted k^{th} mesh patch, and n_k is the number of the points within the patch. In this paper, the segmentation and wireframe generation are implemented with Matlab R2017b.

6
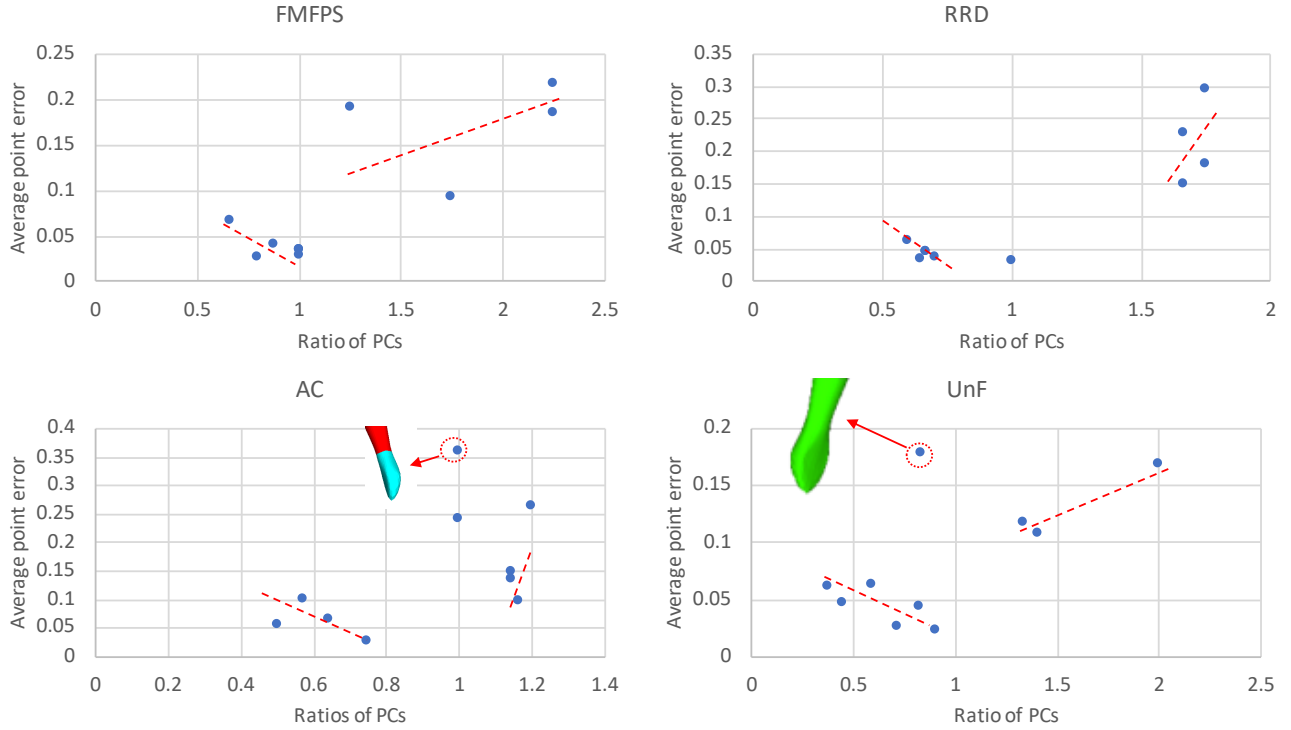
Fig. 6: The correlations of PCA ratio and average point reconstruction error within a patch on 10 patches with four different segmentation methods.

4.1 Dimension ratio of wireframe and mesh patch

This section tests hypothesis 1 that the dimension ratio of boundary wireframe to mesh patch in terms of the number of their corresponding PCs is better to be close to one. To compare different segmentation methods, they are set to produce the same number of mesh patches (i.e., segments). Generally, more patches would lead to a smaller mesh patch size and less variance within each patch. To make the effect of point ratio prominent, the number of patches is set to ten, and the synthesis error of the ten patches are plotted against their dimension ratios in Fig. 6. The error is the average point prediction error within each mesh patch for the ten synthesized human shapes, i.e.,

$$\overline{E}_{mp} = \frac{\sum_{k=1}^{K} E_{mp_k}}{K}$$

where K is the number of synthesized models.

From the correlation results, we can observe several interesting patterns. Firstly, if we divide the charts into two parts by the ratio of one, we can see the points on the right part are generally much higher than those on the left part. This reveals that the ratio smaller than one would lead to a smaller mesh patch synthesis error. As in the synthesis framework, we use the wireframe to predict the mesh patch with the learned relation Υ_k. A ratio larger than one means that the dimension of the boundary wireframe is higher than the mesh patch dimension. In other words, the boundary of a patch has more features than the patch itself. This would

lead to an over-fitting situation and result in a higher prediction error. Secondly, the trend of the data points in the two parts is symmetric to some extent. As can be seen from the figure that there is a decreasing pattern on the left part, and an increasing pattern for the right part. The pattern on the right further verifies that a higher dimension of the boundary wireframe to mesh patch would increase the over-fitting effect. On the contrary, when the ratio is less than one, we can see that the average point prediction error is increased with the decrease of the ratio. This indicates that a lower dimension of the boundary wireframe does not contain enough information to describe a higher dimensional bounded mesh patch in the relation learning. This can also be seen from the outlier points in the AC and the UnF methods. The segmented hand patch only has one wireframe on the wrist, but the hand shape is very different from its boundary. The ratio is not too small in this case because the hand shape is like a cylinder, and the dimension is largely reduced after PCA. Although the dimension ratio of the boundary wireframe to the mesh patch is close to one, such limited wireframe information cannot fully represent the hand patch's full-shaped profile. Therefore the learned relation has a high prediction error. Despite the outliers, the symmetric pattern reveals that the learning performance is generally better with the dimension ratio getting closer to one. However, it may not be the only factor to find an optimal wireframe generation method. The shape difference between the boundary wireframe and the mesh patch should probably be considered too.
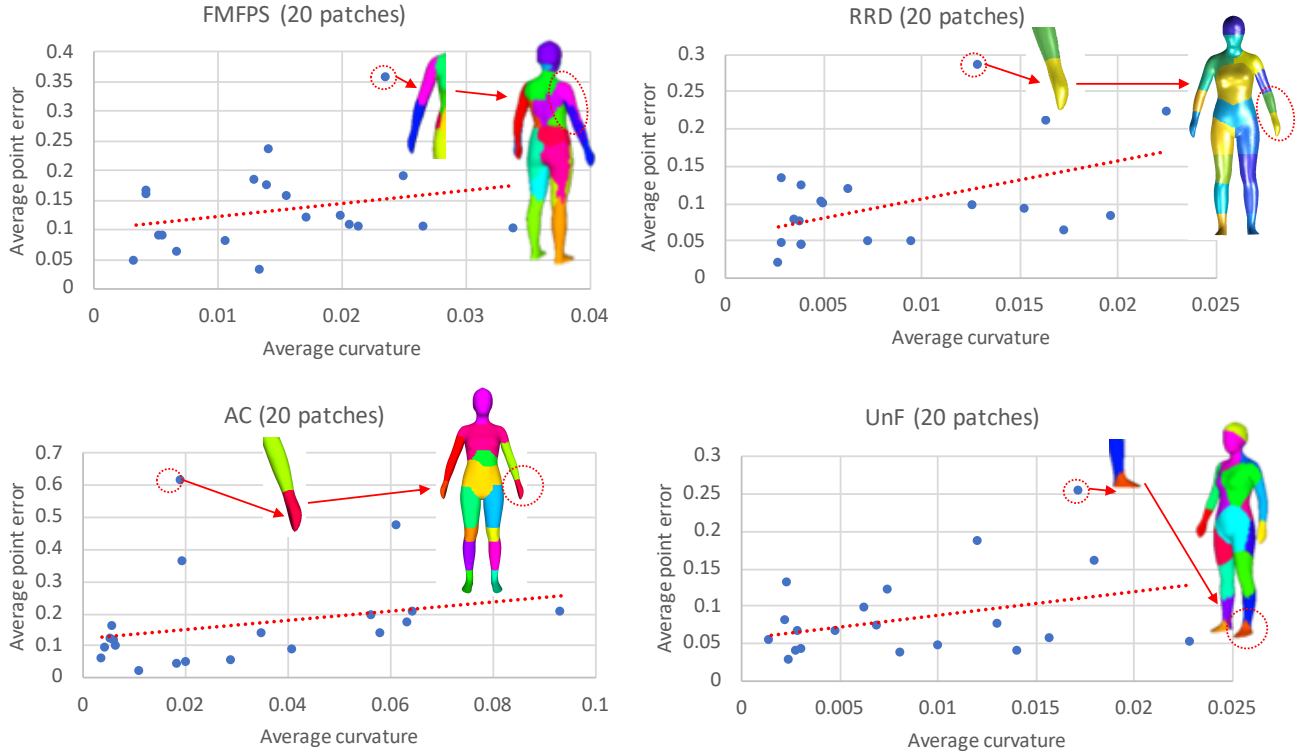
Fig. 7: The correlation between the average curvature of the boundary wireframes and the reconstructed mesh patch error.

4.2 Smoothness of the wireframe

Here, we test hypothesis 2 that a smoother wireframe is beneficial to the learning. To conduct the experiment, firstly, one of the ten synthesized human models is randomly chosen. The reason for using only a single shape is that the models have different shapes and so do the wireframes. The curvatures and errors can vary distinctly model-by-model. Averaging the curvatures and the errors among different models is not meaningful, so a single model is studied instead. The average point prediction errors (Eq.(5)) for each mesh patch is plotted against the curvature of its boundary wireframe, as shown in Fig. 7. As the boundary wireframe has many points and each point has its curvature, all points' average curvature on the boundary wireframe is used here. All four segmentation methods are applied, and the number of segments is set to 20 in this experiment. The segmentation results are also presented in Fig. 7.

It can be seen that with the increasing of the average curvature, the average point error of the synthesized mesh patch presents an increasing pattern, no matter which segmentation method is used. This reveals that the wireframe's curvature indeed influences the relation learning, and generally, a smoother wireframe can lead to better learning performance. Nonetheless, the slope of the increasing line in each segmentation is small. This indicates that the learning performance is not significantly affected by the curvature. Different segmenting rules will lead to totally different wireframes, thus generating various segmented mesh patches. These variances among the patches bring a large variety to the curvature on the wireframes, and this variety also influences the

learning performance. Thus, the pure curvature information on the wireframe cannot represent the entire learning performance, although it can influence the relation learning. This justifies the use of boundary smoothing after segmentation, but it is probably already sufficient for the sake of smoothness. We circled the data points that correspond to the mesh patch with the highest prediction errors. Although different segmentation approaches generate different segmentation results, the patches with the highest errors are located at either the hands/arms or the feet. This further supports the importance of the shape difference between the patch and its boundary.

4.3 Topology of mesh patch

From Hypothesis 3, the topology of the separated mesh patch from the wireframe could affect the learning performance. In this section, the correlation between a mesh patch's topology and the learning performance is studied. As discussed in Section 3.1, the number of closed rings (i.e., the number of closed boundary wireframes) is applied here to estimate the topology of a mesh patch. To study the correlation between the number of closed rings and the learning accuracy, all the ten synthesized models are applied to the comparison. Firstly, we calculated the number of closed boundary wireframes for each mesh patch, separated from the generated wireframes by different segmentation approaches. Then for each synthesized shape, we compute the average predicted point error within the mesh patch through Eq. (5). The average point error within each mesh patch across ten

Copyright © by ASME
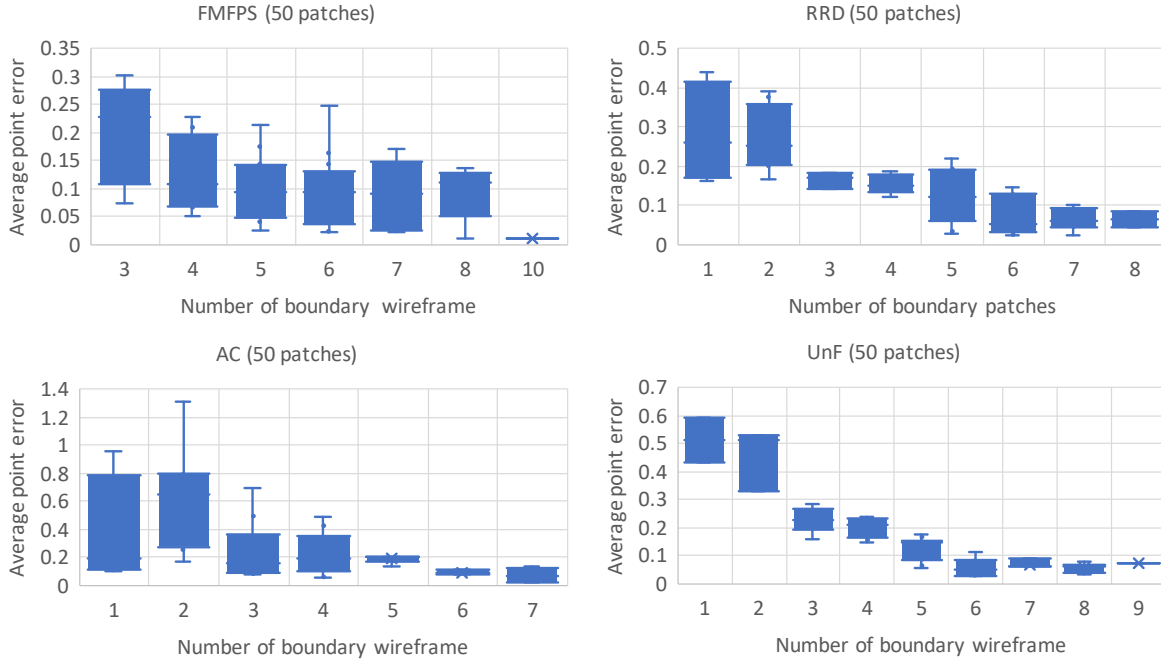
Fig. 8: The correlation between the topology of mesh patch and the reconstructed error.

predicted models are collected, and the correlation between the average point prediction error ($\overline{E}_{mp}$) and the topology are mapped out in a box plot. The number of segments is set to 50 so that there are more boundaries to study the effect of topology.

A clear trend can be observed that with the increasing number of boundary wireframes, the average predicted error decreases. The UnF method has the most apparent pattern that the average error is largely decreased when the mesh patch's number of boundary wireframe is greater or equal to 3. This verifies that a larger number of boundary wireframes can depict a more informative mesh patch contour, which helps learn the relation between the boundary wireframe and the mesh patch. This is mainly because the boundary wireframe serves as the handles. More boundary loops mean more distributed handles throughout the mesh patch, which is more helpful for the learning method to find the relation between the boundary wireframe and mesh patch.

4.4 Uniformity of mesh patches

In this section, we test hypothesis 4 related to the uniformity of patches. A set of wireframes separates the human shape into small mesh patches. It can be seen from Fig. 5 that the sizes of the patches are varied. To see how the mesh patch size variation affects the learning performance, we conduct the uniformity experiment. A randomly chosen shape from the ten synthesized models is applied to conduct this experiment. Firstly, the distribution of the size of segmented mesh patches on this synthesized shape is extracted. Then, each set of mesh patches' uniformity is calculated with Eq.(3). To comprehensively compare the different sets of generated wireframes from four segmentation approaches and see how the different number of resulting separated mesh patches
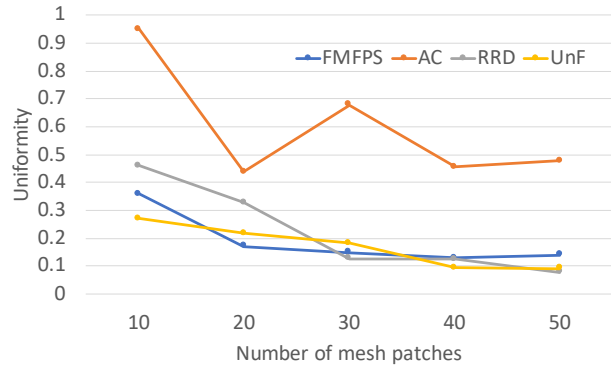
Fig. 9: The correlation between the number of mesh patches and uniformity

would affect the uniformity, we set each segmentation-based wireframe generation approach to produce 10, 20, 30, 40, and 50 mesh patches. For the new synthesized shape, its predicted model error is computed using Eq.(4). We compare the learning performances of different segmentation approach among the different number of mesh patches.

Figure 9 shows the correlation between the number of mesh patches and the uniformity for each segmentation approach. From which it can be seen that with the increasing of the number of segmented patches, the uniformity value decreases, i.e., the variation of the patch size becomes smaller (meaning more uniform). This is an intuitive observation since when we have more patches, each patch's size would be smaller, then the sizes among mesh patches would be closer to each other, and thus the uniformity value would be decreased. It should be noticed that when FMFPS and AC approach increased the mesh patches from 40 to 50, the uni-

<div align="center">9</div>
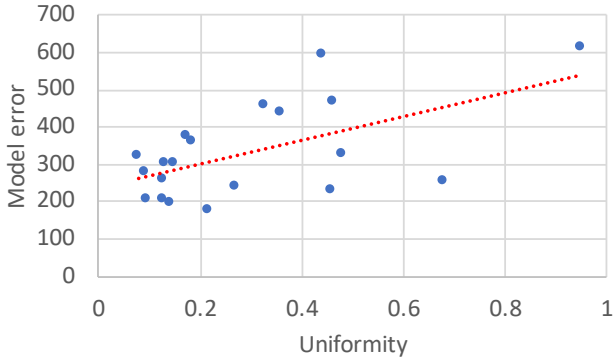
Fig. 10: The correlation between the uniformity and learning performance.

(a)

(b)

Fig. 11: The correlation between the number of mesh patches and reconstructed model error.

formity is slightly increased. This reveals that due to different segmenting principle, the separated mesh patch sizes are not always decreased. For example, in the AC method, the mesh patch needs to satisfy the approximately convex segmenting rule. Although we increased the segmented number of patches, some patches' shape would not always be decreased as it needs to be nearly convex and satisfying other segmenting rules. From this uniformity observation, we can see in general, the segmented mesh patches would be more uniform with the increasing of wireframes, and specific segmenting rules may slightly affect the uniformity value.

We plot the relationship between uniformity and the synthesized model error for the learning performance with different uniformity values. We collect the uniformity of all mesh patches separated from four segmentation approaches and five patch numbers. For all the combinations, the synthesized human shape errors are also collected. Figure 10 is the correlation between the uniformity value and the synthesized human shape error. It can be seen that a larger uniformity value leads to a larger prediction error. This reveals that a more uniformly distributed size of the mesh patches has a small variety. Then the learned relations can better depict the real relationships of the $SP \rightarrow WF$ and $wf_k \rightarrow mp_k$.

4.5 Number of mesh patches

In the previous sections, it can be seen that a different number of patches would lead to different learning accuracy. Therefore, we also study the correlation between the number of mesh patches and the learning performance, and we plot the relationship between the number of mesh patches and predicted model error, as shown in Fig. 11(a). It can be observed when the mesh patches number is less than 50, and there is a trend of more number of mesh patches leading to the smaller predicted mean patch error. Nevertheless, when the mesh patch number reaches 50, it would be slightly increased. This reveals that when using the wireframes separating the human model into small parts, many mesh patches could have the smallest learning error for the human model. Among the methods tested, the optimal number of patches should be around 40. When a different segmentation approach is used to generate the wireframe as the intermediate
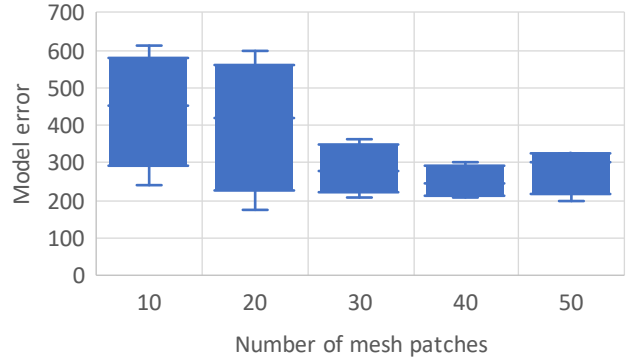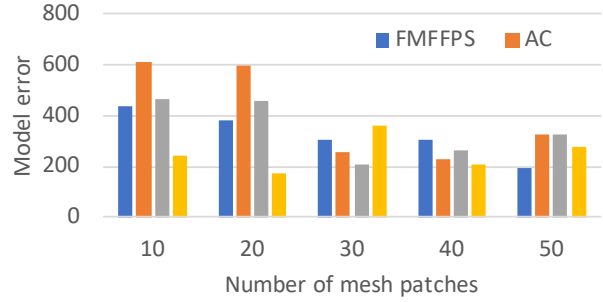
layer for the relation learning, it is suggested to test different segments to find the best learning performance.

If we split such correlation to each segmentation approach, as shown in Fig. 11(b), we can observe that the learning accuracy varies for different segmentation approaches. This is mainly because these segmentation approaches are based on distinct segmenting principles, and the resulting generated wireframes would be diversified, leading to different learning performance. From Fig. 11(b), it can be seen with different segmenting principles, each method has the smallest prediction model error, but the corresponding number of patches varies, e.g., FMFPS is at 50, and UnF is at 20. Generally, FMFPS method performs better on a larger number of patches, and UnF performs better on a smaller number of patches. This is because FMFPS considers curvature, which decreases the feature complexity within a patch. However, it generally results in irregular shapes, so it performs worst when the patch number is low. Nonetheless, the patches will become smaller and more uniform when the patch number is increasing, and thus its performance gets improved. While in the UnF method, with the increasing number of mesh patches, many mesh patches would bring more irregular boundary wireframes even though the mesh patches are distributed more uniformly. This would increase the complexity for learning the relation of $SP \rightarrow WF$, thus worsening the learning performance. Among all the methods, the UnF method performs more steadily with relatively lower errors.

Table 1: Wireframe comparison with manually defining

Wireframe Method	Uniformity	Model Error
Manually defining [7]	0.2815	219.739
FMFPS	0.1296	301.775
AC	0.4561	230.886
RRD	0.1251	261.304
UnF	0.0909	206.445

5 Discussion

From the experimental results in the previous section, it can be seen that the proposed factors are indeed affecting the relation learning performance. However, different segmenting rules would have a distinct influence on the factors. They could also lead to various shapes of each mesh patch, which also seems important. Therefore, to develop a segmentation-based wireframe generation method, the segmenting principle is critical since it directly determines the above criteria. In this section, we firstly compare the automated wireframe generation with the manually defining one, then based on the comparison and the experimental results in Section 4, several design guidelines for the segmentation-based wireframe generating are summarized.

5.1 Comparison to previous work

The segmentation-based wireframe generation is compared with the manual wireframe defining in the previous work [7], which manually defined a wireframe on the human shape based on the anthropocentric rules resulting in 39 mesh patches. To fairly compare with it, the results of the 40-patch generated by the four segmentation approaches are employed here. The uniformity value of these five sets of mesh patches are computed, and the synthesis experiment is conducted. Table 1 shows the results of uniformity and the model error, from which it can be seen that the manually defining method has a relatively larger uniformity value. This is because the manually defining method is based on the knowledge of human shape, and the wireframe does not separate the shape evenly. Also, we can see that the AC approach has a larger uniformity value, mainly because of the AC approach partitions the shape into nearly convex regions. Thus, the resulting size distribution of mesh patches is far from uniform. However, we can see that the model prediction error of manually defining and AC are smaller than FMFPS and RRD. This reveals that although uniformity is an essential factor (UnF has the lowest value of uniformity and model error), if the separated mesh patches include specific meaning or knowledge, the learning performance could be improved. It should be noticed that manually defining takes tedious effort to define a set of meaningful wireframes and usually not available for a new arrival dataset. At the same time, the segmentation-based method can generate wireframes automatically.

From this comparison, we can see it is preferred that a segmenting approach can generate meaningful mesh patch geometry and satisfy the criteria as mentioned earlier for wireframe generation. Besides the aforementioned criteria, other factors also need to be considered. For example, the hand shape appeared many times in the previous experiments. This reveals the difference between the mesh patch and its boundary wireframe needs to be considered when developing a segmentation-based method since the boundary wireframe is used to describe the shape of the mesh patch in the wireframe-assisted learning framework. Besides, how to develop a quantifiable criterion to depict the anthropocentric meaning of the wireframe is another direction. For example, the AC method uses the convexity as such a quantifier: when segmenting the human body shape, a quantifiable and meaningful criterion would be better for the wireframe generation.

5.2 Wireframe design guidelines

It is desired that an automatic and robust wireframe generation methodology can be developed for human body shape learning. Such a wireframe not only provides an intermediate layer for the parametric human body modeling, but it can also be extended for extracting the wireframe network for a three-dimensional digital model. Such a curve network has been widely applied in various applications such as sketch modeling and generative design. Therefore, it is necessary to establish the design guidelines for developing the segmenting principles for generating the expected wireframe of the human body shapes. To develop an automatic wireframe generation method, we conclude the following design guidelines for the segmentation algorithm development based on the experimental studies.

In practice, there could be circumstances that different guidelines have conflicting relationship. For example, more uniformity may lead to less topological variation on simple geometries. Therefore, we rank the guidelines in terms of their impact to the learning performance. For example, the topology criterion is the most preferred since the shape learning is highly dependent on the bounded geometry profile. In contrast, the dimension ratio cannot always guarantee a better learning performance, so it should have a less preference. In the following, we list the design guidelines by their importance and discuss them one by one.

1. More boundary wireframes per mesh patch. It was shown in Section 4.3 that the more closed wireframes in a mesh patch, the lower the learning error. These close boundary loops serve as the handles describing the shape profile of the patch. More closed loops of boundary wireframe are expected for a better relation learning in a mesh patch. Thus, in the segmentation method design, it can be used as a heuristic quantifier to guide the clustering or region growing algorithms.

2. Partition uniformly: From Section 4.4, the learning performance is relevant to the uniformity of the segmented mesh patches. If the knowledge such as the anthropocentric rules of the human shape data is not available, it is expected the size of the resulting mesh patches distributed close to uni-

form. This can be integrated as another designing guideline for the automatic segmentation method developing for wireframe generation.

3. Dimension ratio in the interval [0.8,1.0): It can be seen from Section 4.1 that for most segmentation-based wireframe generation approaches, the dimension ratio of boundary wireframe to mesh patch can affect the relation learning. Without any pre-knowledge of the dataset, it is expected that the dimension ratio is slightly less than one, in the interval [0.8,1.0), when designing a segmenting principle for the wireframe generation. This can be applied as a heuristic principle for the segmentation algorithm designing.

4. As smooth as possible: As it can be seen from Section 4.2 that the smoothness affects the learning performance. Generally, a smaller curvature of the wireframe is expected. This can be deployed as an optimizing criterion when developing a segmentation method for the wireframe generation. It can also be used as a wireframe post-processing guideline, and the wireframe can be processed with a smoothing operator after its generation.

6 Conclusion

In this work, the wireframe automation is studied to replace the manually defining, which was mainly based on anthropocentric experiences. Aiming at develping an automatic wireframe generation method for the human body shape modeling, this paper proposes a segmentation-based wireframe generation methodology. The mesh segmentation is introduced to produce the wireframes on the human body shape. The automation methodology mainly relies on the segmentation algorithm, and thus the quality of the wireframe largely depends on the segmenting principle. This paper studied several quantifiable criteria for evaluating different segmenting principles to evaluate whether the produced wireframe is favorable for wireframe-assisted learning. The quantifiable criteria are used to measure the performance of the methodology. Based on these criteria, the corresponding hypotheses are proposed accordingly. To test the proposed hypotheses, four different segmentation algorithms with unique segmenting principles are applied to produce the wireframe, and the synthesizing experiments are conducted. Experimental results show that most hypotheses are verified, and the criteria are obviously correlated with the learning performance. From the results, several design guidelines and heuristic rules are summarized for the development of a segmentation algorithm to produce wireframes on human body shape. The work's future direction includes the segmentation algorithm development for generating a meaningful wireframe for the human body shape and extraction of knowledge from anthropocentric experiences for wireframe automation.

References

[1] Kwok, T.-H., Zhang, Y.-Q., Wang, C. C., Liu, Y.-J., and Tang, K., 2015. "Styling evolution for tight-fitting garments". *IEEE transactions on visualization and computer graphics,* **22**(5), pp. 1580–1591.

[2] Zhang, Y., and Kwok, T.-H., 2019. "Customization and topology optimization of compression casts/braces on two-manifold surfaces". *Computer-Aided Design,* **111**, pp. 113–122.

[3] Norooz, L., Mauriello, M. L., Jorgensen, A., McNally, B., and Froehlich, J. E., 2015. "Bodyvis: A new approach to body learning through wearable sensing and visualization". In Proceedings of the 33rd Annual ACM Conference on Human Factors in Computing Systems, pp. 1025–1034.

[4] Anguelov, D., Srinivasan, P., Koller, D., Thrun, S., Rodgers, J., and Davis, J., 2005. "Scape: shape completion and animation of people". In *ACM SIGGRAPH 2005 Papers*. pp. 408–416.

[5] Allen, B., Curless, B., and Popović, Z., 2003. "The space of human body shapes: reconstruction and parameterization from range scans". *ACM transactions on graphics (TOG),* **22**(3), pp. 587–594.

[6] Chu, C.-H., Tsai, Y.-T., Wang, C. C., and Kwok, T.-H., 2010. "Exemplar-based statistical model for semantic parametric design of human body". *Computers in Industry,* **61**(6), pp. 541–549.

[7] Huang, J., Kwok, T.-H., and Zhou, C., 2019. "Parametric design for human body modeling by wireframe-assisted deep learning". *Computer-Aided Design,* **108**, pp. 19–29.

[8] Theologou, P., Pratikakis, I., and Theoharis, T., 2015. "A comprehensive overview of methodologies and performance evaluation frameworks in 3d mesh segmentation". *Computer Vision and Image Understanding,* **135**, pp. 49–82.

[9] Rodrigues, R. S., Morgado, J. F., and Gomes, A. J., 2018. "Part-based mesh segmentation: a survey". In Computer Graphics Forum, Vol. 37, Wiley Online Library, pp. 235–274.

[10] Varol, G., Ceylan, D., Russell, B., Yang, J., Yumer, E., Laptev, I., and Schmid, C., 2018. "Bodynet: Volumetric inference of 3d human body shapes". In Proceedings of the European Conference on Computer Vision (ECCV), pp. 20–36.

[11] Hasler, N., Stoll, C., Sunkel, M., Rosenhahn, B., and Seidel, H.-P., 2009. "A statistical model of human pose and body shape". In Computer graphics forum, Vol. 28, Wiley Online Library, pp. 337–346.

[12] Ziaeefard, M., and Bergevin, R., 2015. "Semantic human activity recognition: A literature review". *Pattern Recognition,* **48**(8), pp. 2329–2345.

[13] Cheng, Z.-Q., Chen, Y., Martin, R. R., Wu, T., and Song, Z., 2018. "Parametric modeling of 3d human

body shape—a survey". *Computers & Graphics,* ***71***, pp. 88–100.

[14] Baek, S.-Y., and Lee, K., 2012. "Parametric human body shape modeling framework for human-centered product design". *Computer-Aided Design,* ***44***(1), pp. 56–67.

[15] Seo, H., and Magnenat-Thalmann, N., 2003. "An automatic modeling of human bodies from sizing parameters". In Proceedings of the 2003 symposium on Interactive 3D graphics, pp. 19–26.

[16] Wang, C. C., 2005. "Parameterization and parametric design of mannequins". *Computer-Aided Design,* ***37***(1), pp. 83–98.

[17] KwoK, T.-H., Zhang, Y., and Wang, C. C., 2011. "Efficient optimization of common base domains for cross parameterization". *IEEE Transactions on Visualization and Computer Graphics,* ***18***(10), pp. 1678–1692.

[18] Chen, Y., Liu, Z., and Zhang, Z., 2013. "Tensor-based human body modeling". In The IEEE Conference on Computer Vision and Pattern Recognition (CVPR).

[19] Zhang, Y., Zheng, J., and Magnenat-Thalmann, N., 2015. "Example-guided anthropometric human body modeling". *The Visual Computer,* ***31***(12), pp. 1615–1631.

[20] Hu, R., Fan, L., and Liu, L., 2012. "Co-segmentation of 3d shapes via subspace clustering". In Computer graphics forum, Vol. 31, Wiley Online Library, pp. 1703–1713.

[21] Liu, R., and Zhang, H., 2004. "Segmentation of 3d meshes through spectral clustering". In 12th Pacific Conference on Computer Graphics and Applications, 2004. PG 2004. Proceedings., IEEE, pp. 298–305.

[22] Benhabiles, H., Lavoué, G., Vandeborre, J.-P., and Daoudi, M., 2011. "Learning boundary edges for 3d-mesh segmentation". In Computer Graphics Forum, Vol. 30, Wiley Online Library, pp. 2170–2182.

[23] Zheng, Y., and Tai, C.-L., 2010. "Mesh decomposition with cross-boundary brushes". In Computer Graphics Forum, Vol. 29, Wiley Online Library, pp. 527–535.

[24] Bonneel, N., Coeurjolly, D., Gueth, P., and Lachaud, J.-O., 2018. "Mumford-shah mesh processing using the ambrosio-tortorelli functional". In Computer Graphics Forum, Vol. 37, Wiley Online Library, pp. 75–85.

[25] Lawonn, K., Gasteiger, R., Rössl, C., and Preim, B., 2014. "Adaptive and robust curve smoothing on surface meshes". *Computers & graphics,* ***40***, pp. 22–35.

[26] Schindler, F., and Förstner, W., 2011. "Fast marching for robust surface segmentation". In ISPRS Conference on Photogrammetric Image Analysis, Springer, pp. 147–158.

[27] Kimmel, R., and Sethian, J. A., 1998. "Computing geodesic paths on manifolds". *Proceedings of the national academy of Sciences,* ***95***(15), pp. 8431–8435.

[28] Moenning, C., and Dodgson, N. A., 2003. "Fast Marching farthest point sampling". In Eurographics 2003 - Posters, Eurographics Association.

[29] Dessein, A., Smith, W. A., Wilson, R. C., and Hancock, E. R., 2017. "Symmetry-aware mesh segmentation into uniform overlapping patches". In Computer Graphics Forum, Vol. 36, Wiley Online Library, pp. 95–107.

[30] Kaick, O. V., Fish, N., Kleiman, Y., Asafi, S., and Cohen-Or, D., 2014. "Shape segmentation by approximate convexity analysis". *ACM Transactions on Graphics (TOG),* ***34***(1), pp. 1–11.

[31] Shapira, L., Shamir, A., and Cohen-Or, D., 2008. "Consistent mesh partitioning and skeletonisation using the shape diameter function". *The Visual Computer,* ***24***(4), p. 249.

[32] Rubner, Y., Tomasi, C., and Guibas, L. J., 2000. "The earth mover's distance as a metric for image retrieval". *International journal of computer vision,* ***40***(2), pp. 99–121.

[33] Rodola, E., Bulo, S. R., and Cremers, D., 2014. "Robust region detection via consensus segmentation of deformable shapes". In Computer Graphics Forum, Vol. 33, Wiley Online Library, pp. 97–106.

[34] Golovinskiy, A., and Funkhouser, T., 2008. "Randomized cuts for 3d mesh analysis". In *ACM SIGGRAPH Asia 2008 papers*. pp. 1–12.

[35] Rustamov, R. M., 2007. "Laplace-beltrami eigenfunctions for deformation invariant shape representation". In Proceedings of the fifth Eurographics symposium on Geometry processing, Eurographics Association, pp. 225–233.